Egyptian Journal of Radiology and Nuclear Medicine

CASE REPORT Open Access

Primary sinonasal chondroid chordoma in a pediatric patient: a diagnostic challenge

Prachi Mann[1*], Ayush Arya[1], Amit Disawal[1] and Aarti Anand[1]

Abstract

Background Chordomas are rare, malignant tumors typically centered in midline structures such as the clivus and sacrum, with peak prevalence in the fourth decade. Clival chordomas may secondarily extend to involve the nasopharynx and nasal cavity; however, primary extra-osseous chordomas are even more uncommon. We present an unusual case of a primary sinonasal chondroid chordoma arising from the maxillary sinus in a 5-year-old child. This is the second case of primary sinonasal chordoma reported in the literature so far, after Tao ZZ et al. and the first case of the chondroid variant.

Case presentation A 5-year-old male presented with right-sided nasal obstruction, nasal congestion, and snoring for 2 months. Physical examination showed a reddish polypoidal mass in the right nasal cavity obstructing the choana with nasal septal deviation toward left side. Radiological examination with CT confirmed the presence of a well-defined, heterogeneously hyperdense lobulated mass in right maxillary sinus extending into right nasal cavity with intralesional coarse calcifications. MRI revealed expansile solid altered signal intensity mass, which appears to be isointense on T1-weighted imaging (T1WI) and heterogeneously hyperintense on T2-weighted imaging (T2WI) with a heterogeneous honeycomb pattern of enhancement. Differentials considered were rhabdomyosarcoma, nasopharyngeal carcinoma, and neuroblastoma metastasis. However, the lesion was pathologically proven as a chondroid chordoma. No association with skull base or clival lesion was found on review.

Conclusions Primary sinonasal chordomas are rare in occurrence but should be considered a differential for sinonasal masses in the presence of characteristic MRI features, despite their uncommon location.

Keywords Chondroid chordoma, Extra-osseous chordoma, Sinonasal chordoma, Pediatric sinonasal masses

Background

Chordoma are rare, malignant tumors arising from embryonic remnants of primitive notochord that remain entrapped in midline structures such as the clivus (at spheno-occipital synchondrosis), vertebral bodies, and sacrococcygeal region. These are low-grade, slow growing, but locally invasive tumors with a high recurrence rate and significant mortality. They are generally seen in adults; however, some histological variants are relatively common in the pediatric age group such as the dedifferentiated and chondroid variants [1].

Intracranial clival chordomas typically extend in the direction of the nasopharynx and occasionally into the nasal cavity. Primary extra-osseous chordomas have also been previously reported in the nasal cavity and nasopharynx in the absence of a clival lesion.

We present an unusual case of a primary sinonasal chondroid chordoma arising from the maxillary sinus in a 5-year-old child. This is the second case of primary sinonasal chordoma reported in the literature so far after Tao ZZ et al. [2] and the first case of the chondroid variant.

*Correspondence:
Prachi Mann
mannprachi5@gmail.com
[1] Department of Radiodiagnosis, Government Medical College and Hospital, Nagpur, Ajni Road, Hanuman Nagar, Nagpur 440009, India

Case presentation

A 5-year-old male presented with right-sided nasal obstruction, nasal congestion, and snoring for 2 months. There was a history of facial trauma, i.e., fall over the nose one year ago. There was no history of headaches, epistaxis, or visual disturbances.

Laboratory results revealed a normal hemoglobin of 10.4 g/dl, a platelet count of 301×10^9/L, and leukocyte count of 7.9×10^9/L. Liver and kidney function tests were within the normal range. Coagulation studies showed no abnormality.

The patient was referred to otorhinolaryngology for further evaluation; physical examination was performed, which revealed a reddish polypoidal mass in the right nasal cavity obstructing the posterior choana with nasal septal deviation toward left side. On probe test, there was inability to delineate the lateral wall of right nasal cavity along with a mucoid nasal discharge. There was associated right maxillary and frontal tenderness.

The patient was advised computed tomography of the paranasal sinus (PNS), which confirmed the presence of a well-defined, heterogeneously hyperdense lobulated mass approximately 4×5 cm in the right maxillary sinus extending into the right nasal cavity and ethmoid air cells. There were few intralesional coarse calcifications, with scalloping, thinning, and rarefaction of all walls of right maxillary sinus, the medial wall of right orbit, right pterygoid base, and bony nasal septum (Fig. 1).

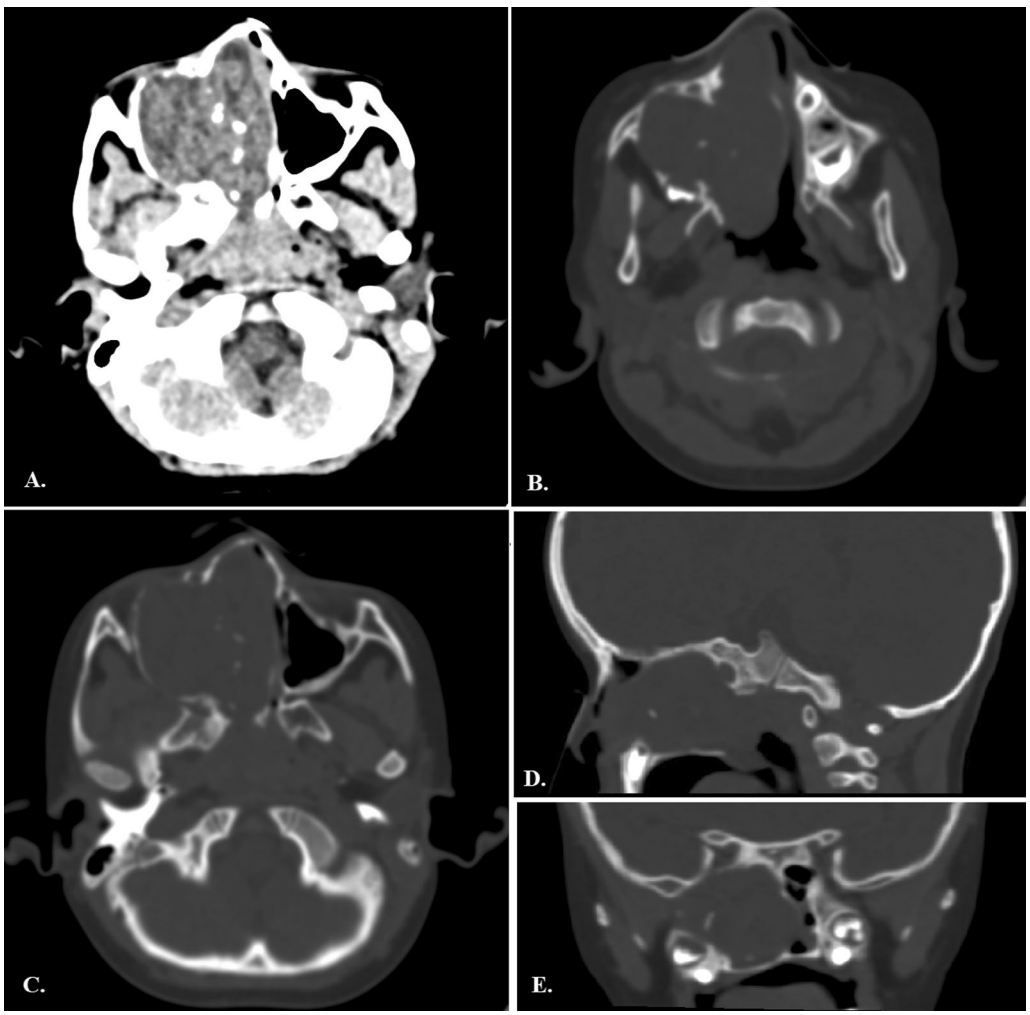

Fig. 1 **A** Axial plain CT of paranasal sinus shows a well-defined, heterogeneously hyperdense mass lesion epicentered in the right maxillary sinus with extension into nasal cavity and coarse calcifications within. **B**, **C** Axial bone window shows rarefaction and expansion of all walls of right maxillary sinus, with deviation of nasal septum toward the left. **D** Sagittal reformatted CT in bone window shows the absence of any lytic lesion in clivus and an unfused spheno-occipital synchondrosis. **E** Coronal reformatted CT image shows downward bowing of the hard palate, without any osseous erosion

Magnetic resonance imaging with contrast was performed, which revealed a well-defined, expansile, solid altered signal intensity mass that appears to be isointense on T1-weighted imaging (T1WI) and heterogeneously hyperintense on T2-weighted imaging (T2WI) without any diffusion restriction. It shows heterogeneous enhancement with areas of low T1 signal intensity within, giving a honeycomb appearance. Few foci of blooming were seen on SWI, which appear hypointense on PHASE sequence, suggestive of calcification (Figs. 2 and 3).

Superiorly, it is extending to involve right ethmoid air cells and reaching up to the cribriform plate. It is displacing the floor of right orbit superiorly; however, no intraorbital or intracranial extension is seen.

Differentials considered were rhabdomyosarcoma, nasopharyngeal carcinoma, and neuroblastoma metastasis.

Gross primary resection of the tumor was done by a right lateral rhinotomy approach. Macroscopically, the tumor tissue was lobulated gray-white tissue that was firm to hard in consistency.

Histopathology of the mass showed lobules of chondroid matrix (predominant) with myxoid and hyaline matrix surrounded by nests, cords, and singly scattered round to polygonal cells having centrally placed hyperchromatic nuclei and moderately eosinophilic to clear cytoplasm. No mitotic activity was seen. The lobules

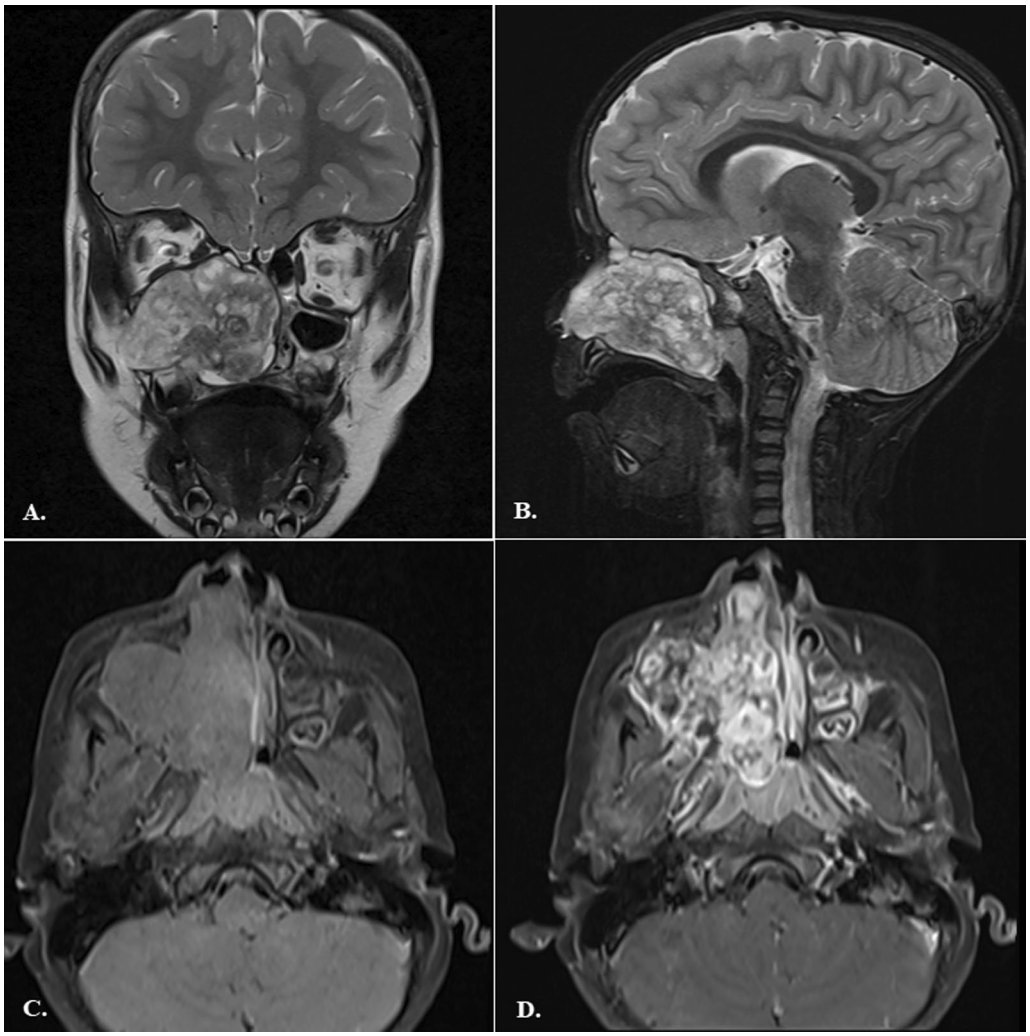

Fig. 2 **A** T2 WI in coronal view shows a heterogeneously hyperintense lesion with T2 hypointense septae within. No intraorbital or intracranial extension was seen. **B** T2 WI in sagittal view shows extension into nasopharynx and close proximity to adenoids. The skull base and clivus appear unremarkable. **C**, **D** Axial T1 WI shows T1 hypointense lesion which shows a honeycomb pattern of enhancement on the post-contrast T1 sequence. No T1 hyperintense areas were seen which excludes recent intralesional hemorrhage

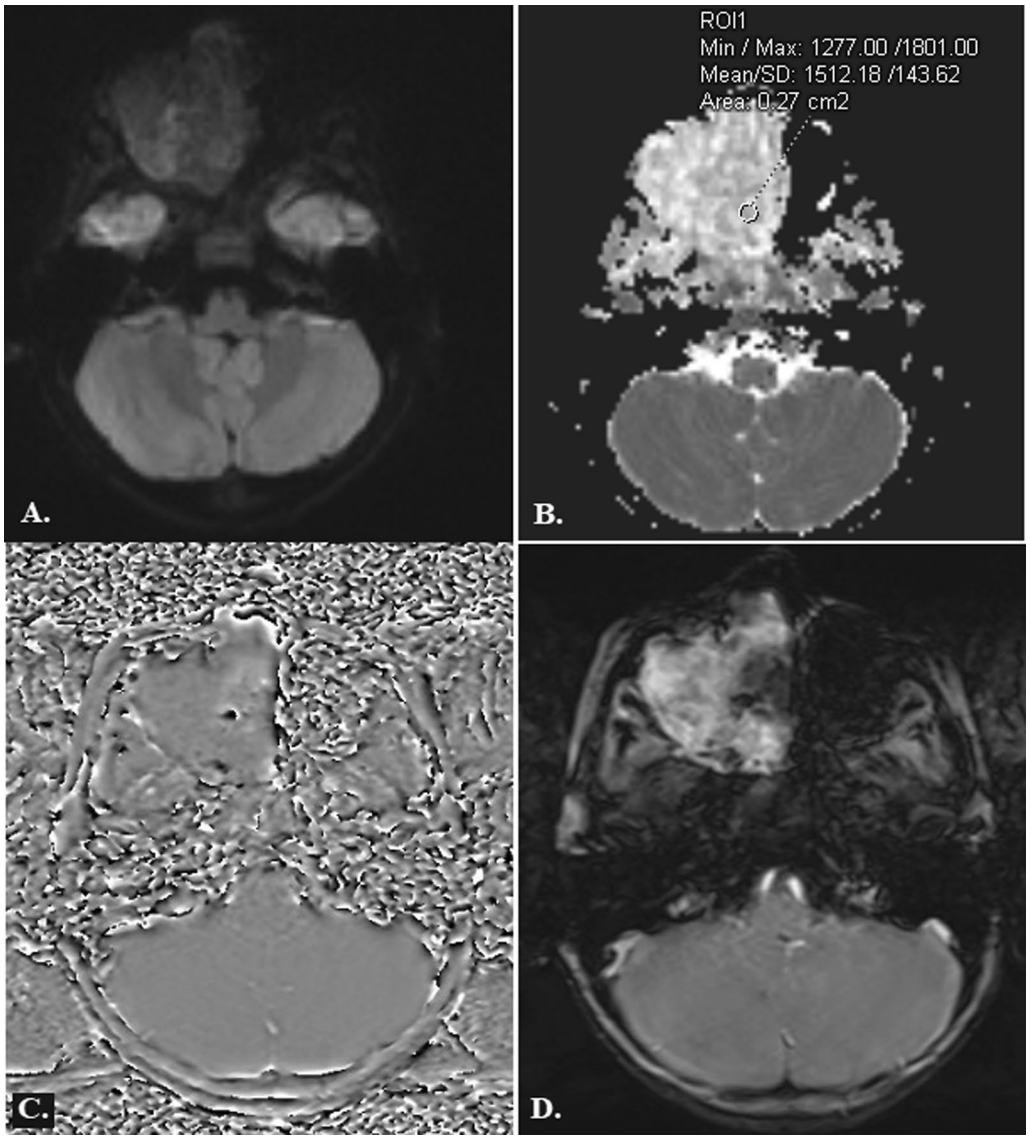

Fig. 3 **A**, **B** Diffusion-weighted image at b1000 shows no areas of restricted diffusion, and ADC values were measured, which favored the signal characteristics of a chordoma. **C**, **D** Few hypointense areas are seen on phase sequence that appear hypointense on magnitude image, consistent with intralesional calcification

were separated by fibrous septae. The histopathological diagnosis was chondroid chordoma (Fig. 4).

Immunohistochemistry revealed positivity for cytokeratin-8/18, S-100, and epithelial membrane antigen (EMA), consistent with chordoma. The patient was started on a radiotherapy regimen for prophylaxis, owing to the high risk of recurrence and mortality.

Discussion

Intracranial chordomas are rare, malignant tumors typically centered at the clivus, with peak prevalence in the fourth decade. They show classical imaging findings, such as being centrally located, well circumscribed, and having an expansile soft tissue mass with lytic destruction of the clivus. Symptoms depend upon structures involved at the skull base, suprasellar, and retroclival extension causing compression over the brainstem, or direct extension into the nasopharynx and nasal cavity [3]. Occurrence at atypical locations such as the nasopharynx, nasal cavity, and paranasal sinus (sphenoid, ethmoid) has been previously documented.

Chordoma can be histologically classified into three variants: [1, 4].

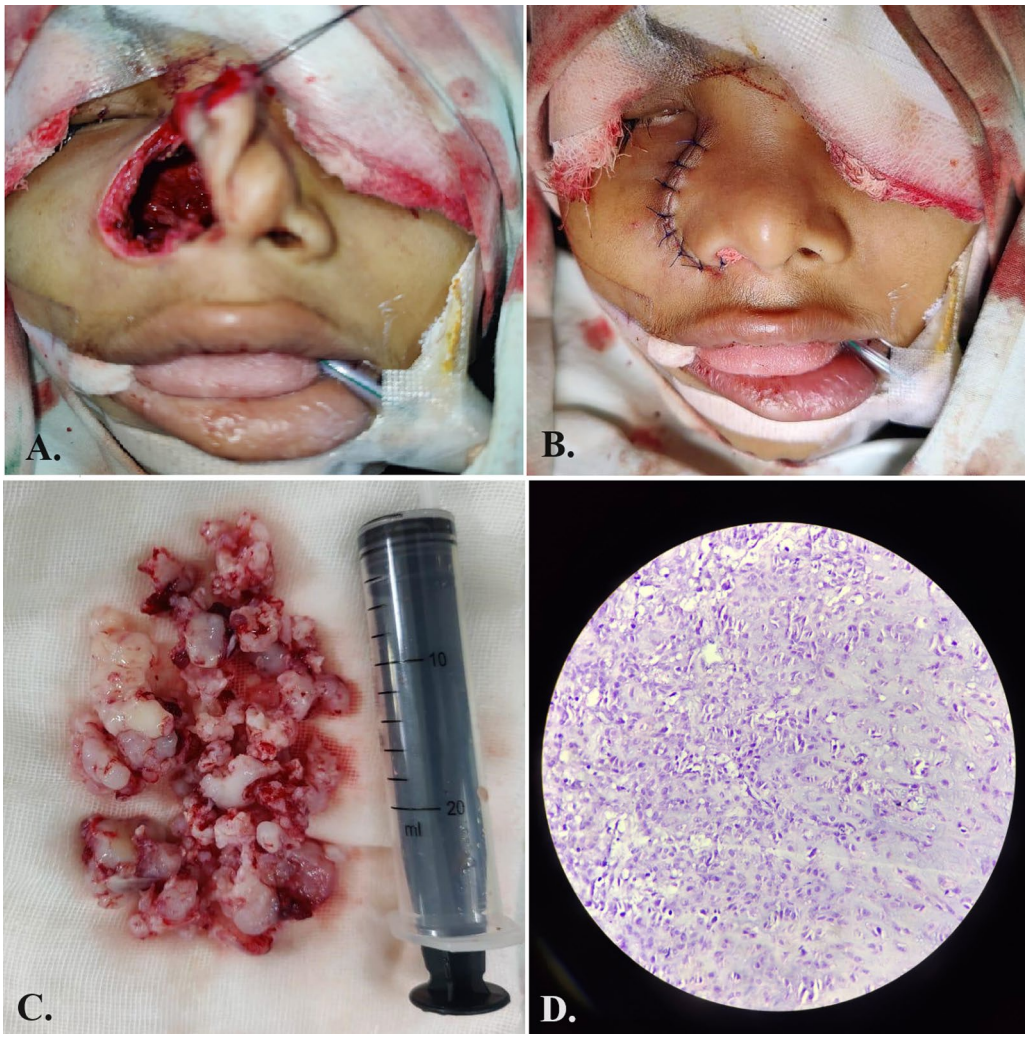

Fig. 4 **A**, **B** Intraoperative image shows a right lateral rhinotomy incision with near total excision of the sinonasal mass lesion. **C** Gross examination shows lobulated gray-white tissue that is firm to hard in consistency. **D** Histopathology image shows nests and cords of round to polygonal cells with centrally placed hyperchromatic nuclei scattered in a chondroid matrix

1. Conventional (classic): most common, may occasionally show areas of dedifferentiation.
2. Dedifferentiated: the most aggressive type and more common in pediatric patients.
3. Chondroid: resembles chondrosarcomas on histopathology due to the presence of myxoid, hyaline stroma. These entities can be differentiated based on immunohistochemistry.

Chordoma and chondrosarcomas have similar imaging appearances; they are both hypointense on T1 WI, heterogeneously hyperintense on T2 WI and show post-contrast enhancement. They can be distinguished based on the relative lateral occurrence of chondrosarcomas at the petro-occipital fissure as compared to chordomas, which are central.

Since our case lacks distinctive features based on age prevalence or lesion location, the utilization of DWI and ADC values becomes helpful to distinguish between the two lesions.

Yeom KW et al. used diffusion-weighted imaging (DWI) to distinguish chordoma and chondrosarcomas by assessing differences in cellular densities and nuclear-to-cytoplasmic ratio based on the motion of water molecules within a tissue voxel. Chondrosarcomas showed higher mean ADC values compared to chordomas. However, ADC may fail as an absolute predictor of diagnosis in cases of histopathological crossover due to variants [5].

Table 1 Imaging differentials of sinonasal mass lesions in pediatric age group

		Features	Imaging features
Non-neoplastic lesions			
1	Antrochoanal polyp	Allergic. Complications due to large stalk, such as torsion, strangulation, auto-amputation, and expulsion	A single polypoidal mass arising from the maxillary sinus extends into the nasal cavity and posterior choana via maxillary ostia (dumbbell shape)
			Highly homogenous signal on T2 with peripheral enhancement
			CT: homogenous opacification and expansion of maxillary sinus [5]
2	Sinonasal polyposis	Asthma and aspirin allergy (Samter's triad)	Multiple polypoidal masses that expand and completely fill sinonasal cavities show a hyperintense signal on T2 with thin peripheral contrast enhancement [5]
		Cystic fibrosis	
3	Rosai-Dorfman disease (Sinus histiocytosis)	Children and adolescents. Most common presentation is bilateral, painless cervical lymphadenopathy. Extranodal disease (43% cases): skin (most common), followed by the paranasal sinuses, nasal cavity, salivary, and lacrimal glands	Multifocal disease, multiple cervical lymph nodes, and extranodal lesions. Isointense on T1, iso- to hypointense on T2, homogenous enhancement [10]
Benign neoplasm			
4	Juvenile nasopharyngeal angiofibroma (JNA)	Adolescent boys present with epistaxis (60% cases). Locally aggressive and highly vascular lesions	Lobulated mass arising at the sphenopalatine foramen with widening and extension into pterygopalatine fossa shows marked post-contrast enhancement with intralesional flow voids [5]
5	Nasal pleomorphic adenoma	Most frequently from nasal septum	Well-circumscribed lobulated mass with peripheral T2 hypointense capsule, heterogeneous contrast enhancement [11]
6	Aneurysmal bone cyst (ABC)	Osteolytic lesion can be primary de novo or secondary to benign tumors such as fibrous dysplasia, central giant cell granuloma, and osteoblastoma	Radiolucent expansile multiloculated masses with a soap bubble appearance. MR imaging: internal thin septae, fluid–fluid levels with septal enhancement [5]
7	Juvenile ossifying fibromas	5–10 years, more aggressive and greater chances of recurrence than their adult counterparts (3–4th decade)	Well-marginated hypodense mass with sclerotic rim and internal lucent areas with mineralized foci. Low to intermediate on T1, heterogeneously hyperintense on T2, with mineralized areas appearing T2 hypointense [5]
		Sharp margins help differentiate from malignant lesions	
8	Sinonasal organized hematoma	History of trauma present	Expansile soft tissue mass, smooth sinus wall erosion, heterogeneous signal intensity with a hypointense peripheral rim on T2-WI images, and marked irregular nodular, papillary, or frond-like enhancement due to neovascularization [12]
Malignant neoplasms			
9	Rhabdomyosarcoma	Bimodal distribution: 2–4 years and 12–16 years of age	Invasive soft tissue mass lesion, iso to hypointense T2, shows restricted diffusion with variable contrast enhancement and central areas of necrosis [13]
		Two histologic variants—embryonal and alveolar (poor prognosis)	
		Associations-Li Fraumeni syndrome, neurofibromatosis type 1	
10	T-cell lymphoma	Epstein–Barr virus, south-east Asia, male predominance. Aggressive lesion with a poor survival rate	Isointense on T1, intermediate on T2, with restricted diffusion and marked contrast enhancement [5]
		Other sites: Waldeyer ring, tonsils, nasopharynx	
		Associated with cervical lymphadenopathy	

Table 1 (continued)

		Features	Imaging features
11	Esthesioneuroblastoma	Rare in children. Bimodal 2nd and 6th decade	Polypoidal lesion epicentered at cribriform plate, causing osseous destruction and intracranial extension with cysts at the brain tumor interface, homogenously enhancing lesion [5]
12	Sinonasal Chordoma	Chordoma, usually at spheno-occipital synchondrosis, sacrococcygeal. Three histologic types: classical, dedifferentiated, and chondroid	Well-defined expansile lobulated mass with T2 hypointense septae and honeycomb pattern of enhancement
		IHC: cytokeratin 8/18, EMA, and S-100 positive. Brachyury-specific	Irregular intratumoral calcifications are seen [2]
13	Chondrosarcoma	Aggressive lesion, paramidline usually at petro-occipital fissure	Similar to chordoma on imaging, differentiated based on location and immunohistochemistry
		IHC: S-100 and vimentin positive	Globular or arc-like calcifications [4]

ADC measurements were obtained to differentiate between chordoma and chondrosarcoma by drawing a region of interest (ROI) manually, excluding areas of calcification, necrosis, and cystic change. Mean, minimum, and maximum ADC values (10 − 6 mm^2/s) obtained, i.e., 1512, 1277, and 1801, respectively, were compared with reference values by Yeom KW et al. for chordoma (1474 ± 117, 905 ± 118 and 2199 ± 255) and chondrosarcoma (2051 ± 262, 1488 ± 360 and 2503 ± 512). The values obtained correspond with the ADC characteristics of a chordoma (Fig. 3B).

While DWI and ADC measurements offer valuable insights into tissue characteristics, their utility may be influenced by technical factors, imaging parameters, and ROI placements, necessitating further validation through additional studies [5].

Sinonasal mass lesions usually manifest with non-specific symptoms such as nasal obstruction, headache, and facial pain, making an accurate diagnosis challenging. Imaging modalities, particularly MRI, play a crucial role in characterization and surgical planning. Primary sinonasal chordomas are rare in occurrence; their key MRI features include a well-defined expansile lobulated mass with T2 hypointense septae along with honeycomb pattern of enhancement. However, it is imperative to consider a broad differential list, as outlined in Table 1, to avoid misdiagnosis [6].

Histopathological examination is the gold standard for a definitive diagnosis. Chondroid chordomas exhibit characteristic lobules of chondroid matrix with myxoid and hyaline components, distinguishable from other chordoma variants and chondrosarcomas through immunohistochemistry markers such as cytokeratin-8/18, S-100, and epithelial membrane antigen (EMA).

The optimal management of primary sinonasal chondroid chordomas involves a multidisciplinary approach comprising surgical resection and adjuvant radiotherapy. A complete en bloc surgical resection remains the cornerstone of treatment, aiming for clear margins while preserving vital structures. High-dose radiation therapy (such as proton beam) is recommended for all histological variants due to the high local recurrence [7, 8].

Chondroid variants were previously believed to have a better prognosis compared to other types; however, according to Almefty K et al. [9], the biologic behavior and outcomes of chondroid chordoma are comparable with the conventional variant, emphasizing the need for vigilant surveillance and long-term follow-up.

Conclusions

Chordomas are the most common primary malignant osseous tumors of the skull base and have typical imaging features. However, in the presence of characteristic imaging features, they should be considered a differential, despite their atypical extra-osseous location.

Teaching points

1. Primary sinonasal chordomas are rare in occurrence but should be considered a differential for sinonasal masses in the presence of characteristic MRI features, despite their uncommon location.
2. Imaging differentials of pediatric sinonasal mass lesions.
3. Role of ADC values in the differentiation of chordomas and chondrosarcomas.

Abbreviations

ADC	Apparent diffusion co-efficient
CT	Computed tomography
EMA	Epithelial membrane antigen
MRI	Magnetic resonance imaging
PNS	Paranasal sinus
ROI	Region of interest
SWI	Susceptibility-weighted images
T2WI	T2-weighted image
T1WI	T1-weighted images
T1FS C +	T1W fat-suppressed post-contrast image

Acknowledgements
NA

Author contributions
All authors read and approved the final manuscript. PM contributed to conceptualization, writing original draft, formal analysis and investigation, and reviewing and editing. AA and AD contributed to validation, visualization, methodology, and data curation. AA contributed to resources, supervision, and writing—reviewing and editing.

Funding
No funding was received for conducting this study.

Availability of data and materials
All data generated or analyzed during this study are included in this manuscript.

Declarations

Ethics approval and consent to participate
Institutional Review Board approval was not required since this was a retrospective observational study. All measures to not disclose the identity of the patient were taken. Only limited sections of the images showing relevant findings were taken, hiding other imaging details.

Consent for publication
Written informed consent was obtained from the patient's relatives.

Competing interests
The authors declare that they have no competing interests.

Received: 26 March 2024 Accepted: 30 May 2024
Published online: 07 June 2024

References

1. Beccaria K, Sainte-Rose C, Zerah M, Puget S (2015) Paediatric chordomas. Orphanet J Rare Dis 10:1

2. Tao ZZ, Chen SM, Liu JF, Huang XL, Zhou L (2005) Paranasal sinuses chordoma in pediatric patient: a case report and literature review. Int J Pediatr Otorhinolaryngol 69(10):1415–1418
3. Yan ZY, Yang BT, Wang ZC, Xian JF, Li M (2010) Primary chordoma in the nasal cavity and nasopharynx: CT and MR imaging findings. Am J Neuroradiol 31(2):246–250
4. Rosenberg AE, Brown GA, Bhan AK, Lee JM (1994) Chondroid chordoma—a variant of chordoma: a morphologic and immunohistochemical study. Am J Clin Pathol 101(1):36–41
5. Yeom KW, Lober RM, Mobley BC, Harsh G, Vogel H, Allagio R, Pearson M, Edwards MS, Fischbein NJ (2013) Diffusion-weighted MRI: distinction of skull base chordoma from chondrosarcoma. Am J Neuroradiol 34(5):1056–1061
6. Rodriguez DP, Orscheln ES, Koch BL (2017) Masses of the nose, nasal cavity, and nasopharynx in children. Radiographics 37(6):1704–1730
7. Tenny S, Varacallo M. Chordoma. InStatPearls [Internet] 2022 Sep 4. StatPearls Publishing.
8. Yamazawa E, Takahashi S, Shin M, Tanaka S, Takahashi W, Nakamoto T, Suzuki Y, Takami H, Saito N (2022) MRI-based radiomics differentiates skull base chordoma and chondrosarcoma: a preliminary study. Cancers 14(13):3264
9. Almefty K, Pravdenkova S, Colli BO, Al-Mefty O, Gokden M (2007) Chordoma and chondrosarcoma: similar, but quite different, skull base tumors. Cancer Interdiscipl Int J Am Cancer Soc 110(11):2467–77
10. LaBarge DV III, Salzman KL, Harnsberger HR, Ginsberg LE, Hamilton BE, Wiggins RH III, Hudgins PA (2008) Sinus histiocytosis with massive lymphadenopathy (Rosai-Dorfman disease): imaging manifestations in the head and neck. Am J Roentgenol. 191(6):W299-306
11. Konsulov S, Milkov D, Markov D, Poryazova EG. Diagnostic challenges of sinonasal pleomorphic adenoma. Cureus. 2024;16(2).
12. Kim EY, Kim HJ, Chung SK, Dhong HJ, Kim HY, Yim YJ, Kim ST, Jeon P, Ko YH (2008) Sinonasal organized hematoma: CT and MR imaging findings. Am J Neuroradiol 29(6):1204–1208
13. Herrmann BW, Sotelo-Avila C, Eisenbeis JF (2003) Pediatric sinonasal rhabdomyosarcoma: three cases and a review of the literature. Am J Otolaryngol 24(3):174–180

Publisher's Note